Taylor & Francis
Taylor & Francis Group

Computer Methods in Biomechanics and Biomedical Engineering

ISSN: 1025-5842 (Print) 1476-8259 (Online) Journal homepage: https://www.tandfonline.com/loi/gcmb20

Modelling 3D control of upright stance using an optimal control strategy

Xingda Qu & Maury A. Nussbaum

To cite this article: Xingda Qu & Maury A. Nussbaum (2012) Modelling 3D control of upright stance using an optimal control strategy, Computer Methods in Biomechanics and Biomedical Engineering, 15:10, 1053-1063, DOI: 10.1080/10255842.2011.570339

To link to this article: https://doi.org/10.1080/10255842.2011.570339

Computer Methods in Biomechanics and Biomedical Engineering
Vol. 15, No. 10, October 2012, 1053–1063

Taylor & Francis
Taylor & Francis Group

Modelling 3D control of upright stance using an optimal control strategy

Xingda Qu[a]* and Maury A. Nussbaum[b]

[a]*School of Mechanical and Aerospace Engineering, Nanyang Technological University, BLK N3, North Spine Nanyang Avenue, Singapore 639798;* [b]*Department of Industrial and Systems Engineering, Virginia Tech, Blacksburg, VA, USA*

(*Received 16 November 2010; final version received 7 March 2011*)

A 3D balance control model of quiet upright stance is presented, based on an optimal control strategy, and evaluated in terms of its ability to simulate postural sway in both the anterior–posterior and medial–lateral directions. The human body was represented as a two-segment inverted pendulum. Several assumptions were made to linearise body dynamics, for example, that there was no transverse rotation during upright stance. The neural controller was presumed to be an optimal controller that generates ankle control torque and hip control torque according to certain performance criteria. An optimisation procedure was used to determine the values of unspecified model parameters including random disturbance gains and sensory delay times. This model was used to simulate postural sway behaviours characterised by centre-of-pressure (COP)-based measures. Confidence intervals for all normalised COP-based measures contained unity, indicating no significant differences between any of the simulated COP-based measures and corresponding experimental references. In addition, mean normalised errors for the traditional measures were $<8\%$, and those for most statistical mechanics measures were $\sim 3-66\%$. On the basis these results, the proposed 3D balance control model appears to have the ability to accurately simulate 3D postural sway behaviours.

Keywords: balance control; 3D model; optimal control strategy; centre-of-pressure; postural sway

1. Introduction

Maintaining upright balance is a major functional ability of humans, and balance control models are common tools to investigate potential underlying mechanisms in this and other circumstances. Many existing balance control models have adopted a single-segment inverted pendulum to model the human body, and have focused on investigating postural sway only in the sagittal plane (e.g. Ishida et al. 1997; Johansson et al. 1988; Maurer and Peterka 2005). In these models, ankle control torque was the only neural output contributing to controlling upright posture. Although a single-segment inverted pendulum body model is applicable in some circumstances, especially when the sway amplitude is small and an ankle strategy dominates (Kuo 1995), some researchers have argued that such an approach is oversimplified (e.g. Alexandrov et al. 2001; Hsu et al. 2007). For example, Hsu et al. (2007) noted that six major joints along the longitudinal axis of the body are coordinated to stabilise the spatial positions of the centre-of-mass (COM) and head during quiet upright stance.

In addition to ankle control torque, hip control torque is also widely accepted as an important neural output to the control of upright posture, and the contribution of hip control torque has been accounted for by adopting a multi-segment inverted pendulum body model (e.g. Kuo 1995; van der Kooij et al. 1999; Fujisawa et al. 2005). However, these models still limit sway motions to the anterior–posterior (A/P) direction. Existing evidence, however, indicates that medial–lateral (M/L) sway is important in some conditions, and that M/L sway measures are able to account for different balance control mechanisms. For example, the mean velocity of postural sway in the M/L direction was found to significantly increase with the application of external load during upright stance (Qu 2010). McClenaghan et al. (1996) reported that significant age-related differences existed in some frequency-domain measures obtained from M/L postural sway. Thus, a simple 2D balance control model that cannot simulate M/L postural sway is not able to sufficiently reflect how humans control upright posture.

The purpose of this study was to develop a balance control model that can accurately simulate postural sway in 3D space. This model is based on an optimal control strategy, and human body dynamics were described by a two-segment inverted pendulum model with two joints representing the ankle and the hip. To simplify (linearise) the model, we assumed that these joints had limited roles, specifically in controlling sway in the A/P and M/L directions, respectively. As such, it was expected that the proposed 3D balance control model could account for both the ankle and hip strategies typically evidenced in upright

*Corresponding author. Email: xdqu@ntu.edu.sg

ISSN 1025-5842 print/ISSN 1476-8259 online

http://dx.doi.org/10.1080/10255842.2011.570339
http://www.tandfonline.com

postural control (Kuo 1995). Performance of the proposed 3D balance control model was evaluated by comparing model simulations and experimental data for selected measures derived from centre-of-pressure (COP) time series. We hypothesised that this model, including assumptions regarding the contributions of ankle and hip joints, would be sufficient to characterise human behaviours during quiet upright stance, as evidenced by a lack of significant differences between any of the simulated COP-based measures and corresponding experimental references.

2. Methods

Expanding on our prior work (Qu et al. 2007, 2009; Qu and Nussbaum 2009a, 2009b), we described human body dynamics in the model by a two-segment inverted pendulum in 3D space. Sensory systems were assumed to provide accurate ankle and hip angles to the neural controller but with an inherent time delay due to sensory processing, transduction and transmission (van der Kooij et al. 1999). The neural controller was an optimal controller that can minimise a performance index defined by physical quantities relevant to sway in both the A/P and M/L directions. An optimisation procedure using heuristic search approaches was performed to determine unspecified model parameters, such as sensory delay times at the ankle and hip joints. Confidence intervals (95%) of normalised simulated COP-based measures and normalised errors between simulated and experimental COP-based measures were determined and used to evaluate the proposed model in terms of its ability to simulate postural sway.

2.1 Postural control system

The postural control system model is illustrated in Figure 1, in which three portions comprise the closed loop: (1) the neural controller, (2) human body dynamics and (3) sensory systems. Models of each of the three parts are discussed in more detail in subsequent sections. In addition, random disturbance torques were added to the ankle control torque and hip control torque generated by the neural controller to drive sway motions.

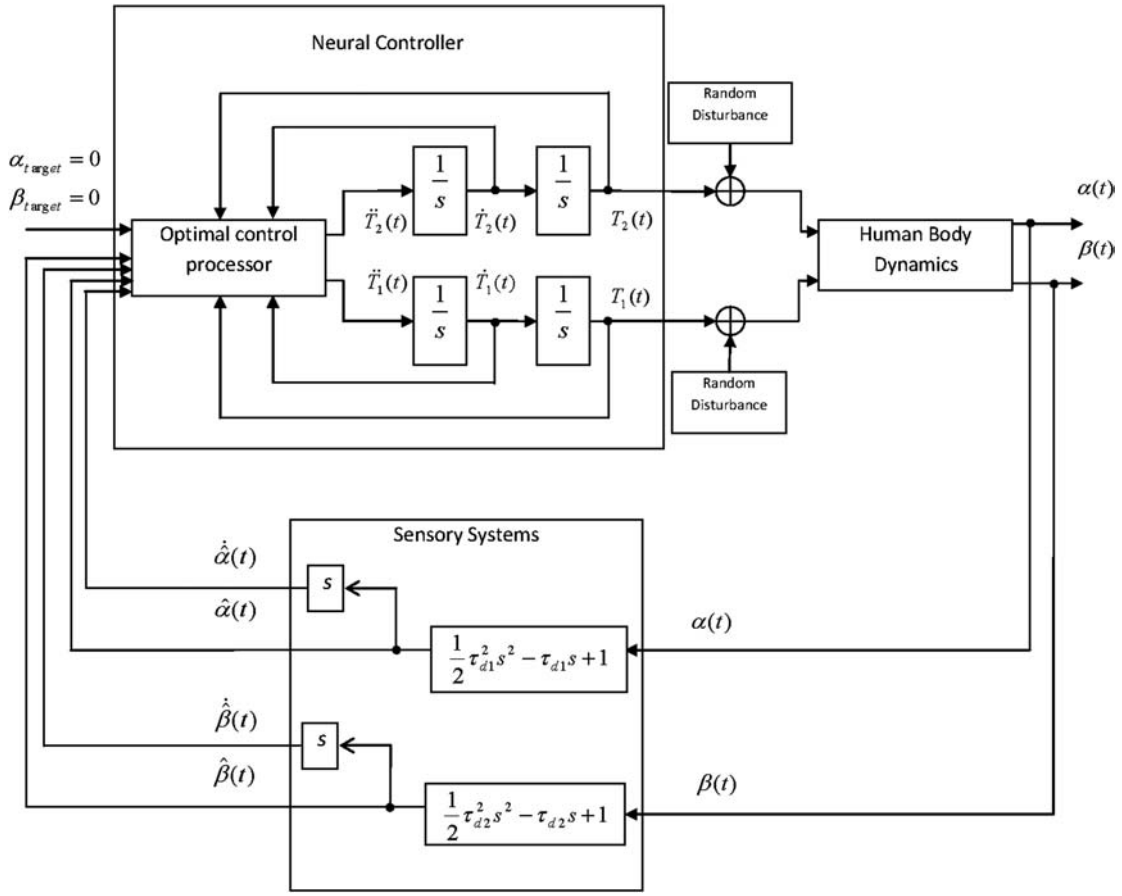

Figure 1. Postural control system for the 3D balance control model. T_1 represents ankle control torque; T_2, hip control torque; α, ankle sway angle; β, hip sway angle; τ_{d1}, sensory delay time at the ankle; and τ_{d2}, sensory delay time at the hip.

2.2 Human body dynamics and sensory systems

A two-segment inverted pendulum in 3D space was used to describe human body dynamics (Figure 2). The two rigid linked segments represent the legs and upper body, respectively; the joint connecting them corresponds the hip joint.

In essence, the dynamics of this two-segment inverted pendulum are nonlinear, yet optimal control formulations are only applicable to linear control systems (though nonlinear optimal control theories have been proposed, these theories are not well formulated and cannot provide global optimal solutions). Given this, some assumptions were required in order to linearise the dynamics. McClenaghan et al. (1996) and Winter et al. (1996) have suggested that the ankle and hip strategies are applied primarily to control postural sway in the sagittal and frontal planes, respectively. Thus, the lower segment (legs), controlled primarily by ankle torques, was assumed to rotate in the sagittal plane (along the A/P direction). Similarly, the upper segment (upper body), controlled primarily by hip torques, was assumed to rotate in the frontal plane (along the M/L direction). In addition, transverse rotations of these two segments were ignored, because such movements are likely minimal during quiet upright stance (Gunther et al. 2008).

Figure 3 illustrates the force analysis of the two-segment inverted pendulum model, in which the *X*-axis is positive to the anterior direction, *Y*-axis is positive to the left and *Z*-axis is positive in the superior direction. According to this, and the above assumptions, the equations of motion are given below; Equations (1)–(3) correspond to a respective force analysis of the upper segment, lower segment and feet, respectively.

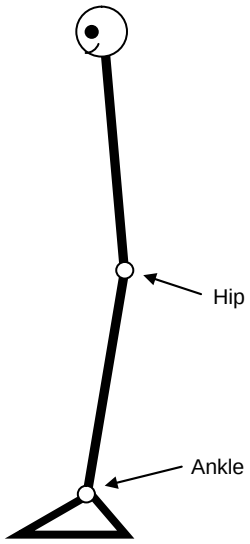

Figure 2. A two-segment inverted pendulum model. *X*-axis is positive in the anterior direction; *Y*-axis is positive to the left and *Z*-axis is positive in the superior direction.

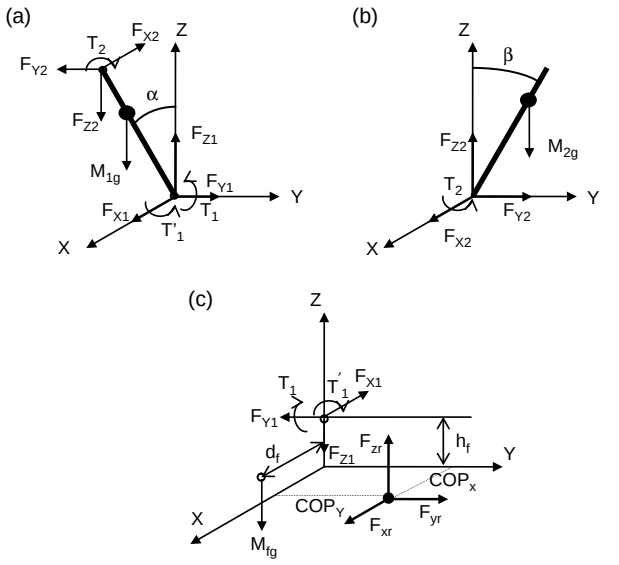

Figure 3. (a) Force analysis of lower segment; (b) force analysis of upper segment and (c) force analysis of foot.

$$\begin{cases} I_2\ddot{\beta} = T_2 - m_2 g Y_{\mathrm{COM2}} \\ F_{Z2} - m_2 g = m_2 \ddot{Z}_{\mathrm{COM2}} \\ F_{Y2} = m_2 \ddot{Y}_{\mathrm{COM2}} \\ F_{X2} = m_2 \ddot{X}_{\mathrm{hip}} \end{cases}, \tag{1}$$

$$\begin{cases} I_1\ddot{\alpha} = T_1 + F_{Z2}X_{\mathrm{hip}} + m_1 g X_{\mathrm{COM1}} - F_{X2}Z_{\mathrm{hip}} \\ T_1^{'} + F_{Y2}Z_{\mathrm{hip}} = T_2 \\ F_{Z1} - F_{Z2} - m_1 g = m_1 \ddot{Z}_{\mathrm{COM1}} \\ F_{Y1} - F_{Y2} = 0 \\ F_{X1} - F_{X2} = m_1 \ddot{X}_{\mathrm{COM1}} \end{cases}, \tag{2}$$

$$\begin{cases} F_{Zr} = F_{Z1} + m_f g \\ F_{Xr} = F_{X1} \\ F_{Yr} = F_{Y1} \\ F_{Zr}\mathrm{COP}_Y + F_{Yr}h_f = T_1^{'} \\ -F_{Zr}\mathrm{COP}_X - F_{Xr}h_f - T_1 + m_f g d_f = 0 \end{cases}, \tag{3}$$

where α is the sway angle of the lower segment in the sagittal plane, β is the sway angle of the upper segment in the frontal plane, I_1 and I_2 are the respective moments of inertia of the lower segment and upper segment, m_1 and m_2 are the respective masses of the lower segment and upper segment, m_f is the mass of the feet, h_f is the height of the ankle, d_f is the horizontal distance between the ankle and the COM of the feet, T_1 is the ankle control torque along the *Y*-axis, $T_1^{'}$ is the ankle control torque along the *X*-axis,

T_2 is the hip control torque along the X-axis, $\{F_{X1}, F_{Y1}, F_{Z1}\}$, $\{F_{X2}, F_{Y2}, F_{Z2}\}$ and $\{F_{Xr}, F_{Yr}, F_{Zr}\}$ are the reaction forces on the ankle, hip and ground, respectively. $\{X_{\mathrm{COM1}}, Y_{\mathrm{COM1}}, Z_{\mathrm{COM1}}\}$, $\{X_{\mathrm{COM2}}, Y_{\mathrm{COM2}}, Z_{\mathrm{COM2}}\}$ and $\{X_{\mathrm{hip}}, Y_{\mathrm{hip}}, Z_{\mathrm{hip}}\}$ are the respective coordinates of the COM of lower segment (COM1), COM of upper segment (COM2) and the hip.

There is no hip torque about the Y-axis, because the upper segment was assumed to rotate in the frontal plane. According to these equations, the COP location is given by

$$\mathrm{COP}_X = \frac{-(m_2\ddot{X}_{\mathrm{hip}} + m_1\ddot{X}_{\mathrm{COM1}})\,h_f - I_1\ddot{\alpha} + (m_2 g + m_2\ddot{Z}_{\mathrm{COM2}})X_{\mathrm{hip}} + m_1 g X_{\mathrm{COM1}} - m_2\ddot{X}_{\mathrm{hip}}Z_{hip} + m_f g \mathrm{d}_f}{(m_1 + m_2 + m_f)g + m_2\ddot{Z}_{\mathrm{COM2}} + m_1\ddot{Z}_{\mathrm{COM1}}}, \tag{4}$$

$$\mathrm{COP}_Y = \frac{I_2\ddot{\beta} + m_2 g Y_{\mathrm{COM2}} - m_2\ddot{Y}_{\mathrm{COM2}}(Z_{\mathrm{hip}} + h_f)}{(m_1 + m_2 + m_f)g + m_2\ddot{Z}_{\mathrm{COM2}} + m_1\ddot{Z}_{\mathrm{COM1}}}. \tag{5}$$

As it was assumed that the lower segment and the upper segment are restricted to rotations in the sagittal and frontal planes, respectively, ankle torque $T_1^{'}$ can be determined by T_1 and T_2. Similarly, the force components in Equations (1)–(3) can also be determined by T_1 and T_2. Thus, according to the assumptions made above, the neural controller only actively generates joint torques T_1 and T_2 to maintain balance and the properties of human body dynamics can be formulated as

$$\begin{cases} I_2\ddot{\beta} = T_2 - m_2 g Y_{\mathrm{COM2}} \\ I_1\ddot{\alpha} = T_1 + F_{Z2}X_{\mathrm{hip}} + m_1 g X_{\mathrm{COM1}} - F_{X2}Z_{\mathrm{hip}}. \end{cases} \tag{6}$$

In addition, the coordinates of the COM1, COM2, hip and ankle are given by

$$\begin{cases} X_{\mathrm{COM1}} = h_1 \times sin\,\alpha; Y_{\mathrm{COM1}} = Y_{ankle}; Z_{\mathrm{COM1}} = h_1 \times \cos\alpha; \\ X_{\mathrm{COM2}} = X_{\mathrm{hip}}; Y_{\mathrm{COM2}} = -h_2 \times \sin\beta; Z_{\mathrm{COM2}} = Z_{\mathrm{hip}} + h_2 \times cos\,\beta; \\ X_{\mathrm{hip}} = l_1 \times sin\,\alpha; Y_{\mathrm{hip}} = Y_{\mathrm{ankle}}; Z_{\mathrm{hip}} = l_1 \times cos\,\alpha; \\ X_{\mathrm{ankle}} = 0; Y_{\mathrm{ankle}} = 0; Z_{\mathrm{ankle}} = 0; \end{cases} \tag{7}$$

where h_1 is the distance of the COM1 relative to the ankle, h_2 is the distance of COM2 relative to the hip, l_1 is the length of lower segment and l_2 is the length of upper segment. We are only interested in spontaneous sway, during which sway angles α and β are very small. Thus, in order to linearise human body dynamics, the following approximations were made: $\sin\alpha \approx \alpha$, $\sin\beta \approx \beta$, $\cos\alpha \approx 1$ and $\cos\beta \approx 1$. Given this, the linear human body dynamics were described as

$$\begin{cases} I_2\ddot{\beta} = T_2 + m_2 g h_2 \beta \\ I_1\ddot{\alpha} = T_1 + m_2 g l_1 \alpha + m_1 g h_1 \alpha - m_2 l_1^2\ddot{\alpha}. \end{cases} \tag{8}$$

Sensory systems were assumed to provide accurate ankle and hip angles to the neural controller but with an inherent time delay due to sensory processing, transduction and transmission (van der Kooij et al. 1999). We also assumed that the time delay was time–invariant for a given individual. To linearise the sensory systems, delayed joint angles $\hat{\alpha}$ and $\hat{\beta}$ were approximated using the first three terms of the Taylor series

$$\begin{aligned} \hat{\alpha}(t) &\approx \alpha(t) - \tau_{d1}\dot{\alpha}(t) + \frac{1}{2}\tau_{d1}^2\ddot{\alpha}(t) \;\; and \\ \hat{\beta}(t) &\approx \beta(t) - \tau_{d2}\dot{\beta}(t) + \frac{1}{2}\tau_{d2}^2\ddot{\beta}(t), \end{aligned} \tag{9}$$

where τ_{d1} and τ_{d2} are the time–invariant delays for the ankle and hip joints, respectively.

Thus, the state Equation (10) that represent the properties of both body dynamics and sensory systems were derived from Equations (8) and (9)

$$\dot{x}(t) = Ax(t) + \mathrm{Bu}(t), \tag{10}$$

where

$$A = \begin{pmatrix} 0 & 1 & 0 & 0 & 0 & 0 & 0 & 0 \\ \frac{m_2 g l_1 + m_1 g h_1}{I_1 + m_2 l_1^2} & 0 & \frac{1}{I_1 + m_2 l_1^2} & \frac{-\tau_{d1}}{I_1 + m_2 l_1^2} & 0 & 0 & 0 & 0 \\ 0 & 0 & 0 & 1 & 0 & 0 & 0 & 0 \\ 0 & 0 & 0 & 0 & 0 & 0 & 0 & 0 \\ 0 & 0 & 0 & 0 & 0 & 1 & 0 & 0 \\ 0 & 0 & 0 & 0 & \frac{m_2 g h_2}{I_2} & 0 & \frac{1}{I_2} & \frac{-\tau_{d2}}{I_2} \\ 0 & 0 & 0 & 0 & 0 & 0 & 0 & 1 \\ 0 & 0 & 0 & 0 & 0 & 0 & 0 & 0 \end{pmatrix},$$

$$B = \begin{pmatrix} 0 & 0 \\ \frac{\tau_{d1}^2}{2(I_1 + m_2 l_1^2)} & 0 \\ 0 & 0 \\ 1 & 0 \\ 0 & 0 \\ 0 & \frac{\tau_{d2}^2}{2I_2} \\ 0 & 0 \\ 0 & 1 \end{pmatrix},$$

the state is

$$x(t) = \begin{pmatrix} \hat{\alpha} \\ \dot{\hat{\alpha}} \\ T_1 \\ \dot{T}_1 \\ \hat{\beta} \\ \dot{\hat{\beta}} \\ T_2 \\ \dot{T}_2 \end{pmatrix}$$

and the control signal is

$$u(t) = \begin{pmatrix} \ddot{T}_1 \\ \ddot{T}_2 \end{pmatrix}.$$

According to Equations (8) and (9), sway angles α and β do not interact with each other, indicating that, based on the assumptions we made above, sway motions in the sagittal plane and frontal plane are independent. As such, the state Equation (10) can be decomposed into two separate state equations that account for the properties of body dynamics in the A/P (Equation (11)) and M/L (Equation (12)) directions.

$$\dot{x}_1(t) = A_1 x_1(t) + B_1 u_1(t), \tag{11}$$

where

$$A_1 = \begin{pmatrix} 0 & 1 & 0 & 0 \\ \frac{m_2 g l_1 + m_1 g h_1}{I_1 + m_2 l_1^2} & 0 & \frac{1}{I_1 + m_2 l_1^2} & \frac{-\tau_{d1}}{I_1 + m_2 l_1^2} \\ 0 & 0 & 0 & 1 \\ 0 & 0 & 0 & 0 \end{pmatrix}, \quad B_1 = \begin{pmatrix} 0 \\ \frac{\tau_{d1}^2}{2(I_1 + m_2 l_1^2)} \\ 0 \\ 1 \end{pmatrix},$$

the state is

$$x_1(t) = \begin{pmatrix} \hat{\alpha} \\ \dot{\hat{\alpha}} \\ T_1 \\ \dot{T}_1 \end{pmatrix} \text{ and the control signal is } u_1(t) = \left(\ddot{T}_1\right).$$

$$\dot{x}_2(t) = A_2 x_2(t) + B_2 u_2(t) \tag{12}$$

where

$$A_2 = \begin{pmatrix} 0 & 1 & 0 & 0 \\ \frac{m_2 g h_2}{I_2} & 0 & \frac{1}{I_2} & \frac{-\tau_{d2}}{I_2} \\ 0 & 0 & 0 & 1 \\ 0 & 0 & 0 & 0 \end{pmatrix}, \quad B = \begin{pmatrix} 0 \\ \frac{\tau_{d2}^2}{2I_2} \\ 0 \\ 1 \end{pmatrix},$$

the state is

$$x(t) = \begin{pmatrix} \hat{\beta} \\ \dot{\hat{\beta}} \\ T_2 \\ \dot{T}_2 \end{pmatrix} \text{ and the control signal is } u_2(t) = \left(\ddot{T}_2\right).$$

2.3 Anthropometry estimation

Different anthropometric data are required to implement this model vs. those required in our earlier 2D model (Qu and Nussbaum 2009a, 2009b). Specifically, the 3D balance control model requires: the moment of inertia of the lower segment around the ankle (I_1), the mass of the lower segment (m_1), the length of the lower segment (l_1) and the length of the COM of the lower segment relative to the ankle (h_1), the moment of inertia of the upper body around the hip (I_2), the mass of the upper body (m_2), the length of the upper body (l_2), the length of the COM of the upper segment relative to the hip (h_2), the mass of the feet (m_F), the height of the ankle (h_F) and the distance between the ankle and the COM of the feet (d_F). Following existing approaches (Der Leva 1996; Chaffin et al. 1999; Robertson et al. 2004), these anthropometric data were obtained by

$$\begin{cases} m_1 = M \times (0.0435 + 0.1027) \times 2,\ m_2 = M \times 0.6708, \\ l_1 = l \times (0.530 - 0.039),\ l_2 = l \times (1 - 0.530), \\ h_1 = l_1 \times 0.6179,\ h_2 = l_2 \times 0.374, \\ I_1 = m_1 \times (l_1 \times 0.650)^2,\ I_2 = m_2 \times (l_2 \times 0.620)^2, \\ m_F = M \times 0.0137 \times 2\,(\text{male})\ \ or\ \ m_F = M \times 0.0129 \times 2\,(\text{female}), \\ h_F = l \times 0.039, \\ d_F = l_F \times 0.4415\,(\text{male})\ \ or\ \ d_F = l_F \times 0.4014\,(\text{female}). \end{cases} \tag{13}$$

2.4 Neural controller

The neural controller (Figure 1) includes an optimal control processor and several integration units. The optimal control processor (Figure 4) is defined by optimal feedback gains. As sway motions in the sagittal and frontal planes are independent, we calculated the optimal feedback for state Equations (11) and (12) separately.

Performance indices for sway motions in the sagittal and frontal planes are defined by Equations (14) and (15), respectively.

$$J_1 = \frac{1}{2}\int_0^\infty (w_{11}\hat{\alpha}^2(t) + w_{21}\dot{\hat{\alpha}}^2(t) + w_{31}T_1^2(t) + w_{41}\dot{T}_1^2(t) + w_{51}\ddot{T}_1^2(t))\mathrm{d}t, \tag{14}$$

$$J_2 = \frac{1}{2}\int_0^\infty (w_{12}\hat{\beta}^2(t) + w_{22}\dot{\hat{\beta}}^2(t) + w_{32}T_2^2(t) + w_{42}\dot{T}_2^2(t) + w_{52}\ddot{T}_2^2(t))\mathrm{d}t, \tag{15}$$

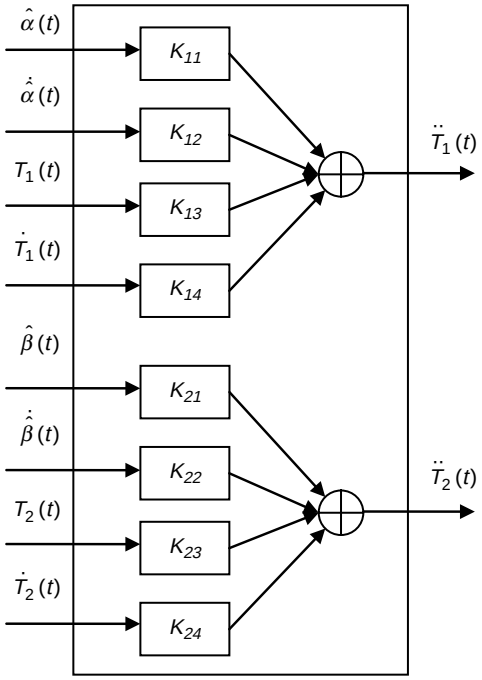

Figure 4. Optimal control processor.

where w_{ij} ($i = 1–5$, $j = 1$ and 2) are weightings of physical quantities relevant to sway. Converting the above performance indices into standard form yields weighting matrices as follows:

$$Q_1 = \begin{pmatrix} w_{11} & 0 & 0 & 0 \\ 0 & w_{21} & 0 & 0 \\ 0 & 0 & w_{31} & 0 \\ 0 & 0 & 0 & w_{41} \end{pmatrix} \text{ and } R_1 = w_{51}, \quad (16)$$

$$Q_2 = \begin{pmatrix} w_{12} & 0 & 0 & 0 \\ 0 & w_{22} & 0 & 0 \\ 0 & 0 & w_{32} & 0 \\ 0 & 0 & 0 & w_{42} \end{pmatrix} \text{ and } R_2 = w_{52}. \quad (17)$$

Note that as long as J_1 and J_2 are minimised, the sum of J_1 and J_2 must be also minimised. Therefore, we were able to calculate the optimal feedback gains for sway motions in the A/P and M/L directions separately and still optimise the performance of the complete postural control system.

2.5 Model specification

An optimisation procedure was used to specify model parameters, including weights of relevant physical quantities, random disturbance gains and sensory delay times. As the model simulates postural sway in both the A/P and M/L directions, the cost function should be defined by sway measures in both directions. We chose two time-domain COP-based measures and two frequency-domain COP-based measures. All are 'traditional' measures (Norris et al. 2005), specifically root mean square displacement (A/P RMS and M/L RMS), mean velocity (A/P MV and M/L MV), centroidal frequency (A/P CFREQ and M/L CFREQ) and frequency dispersion (A/P FREQD and M/L FREQD). The cost function is defined as

$$E = \sum_{i=1}^{N} \left(\frac{\mathrm{COPM}_i - \hat{\mathrm{COPM}}_i}{\hat{\mathrm{COPM}}_i} \right)^2, \quad (18)$$

where $N = 8$ is the number of COP-based measures, and COPM_i and $\hat{\mathrm{COPM}}_i$ are the ith COP-based measure from the simulation and experimental results, respectively. A genetic algorithm (GA) and simulated annealing (SA) were used to specify model parameters, i.e. to minimise E (Hillier and Lieberman 2005). In the GA, the number of chromosomes in a generation was set at 140; the crossover rate and mutation rate were set at 0.80–0.90 and 0.05–0.10, respectively, according to the generation number, and the maximum number of generations was set at 90. In SA, the temperature was initialised at 30% of the initial cost function, the cooling rate was set at 0.80, the number of iterations between temperature changes was set at 40 and maximum number of iterations was set at 200. These values were determined from trial and error. Note that as both the GA and SA were heuristic approaches, the solution obtained from the optimisation procedure cannot be guaranteed to be globally optimal.

2.6 Participants and experimental procedures

Experimental data (COP time series) were required to specify model parameters. These data were a subset obtained from eight male and eight female participants (18–24 years) in a prior study (Lin et al. 2009). Briefly, COP time series were obtained in the A/P and M/L direction, during trials of quiet upright stance, both before and after exercises to induce localised muscle fatigue (LMF). A commercial dynamometer (Biodex Medical Systems, Shirley, NY, USA) was used to induce LMF in the ankle plantar flexors (ankle fatigue) and lumbar extensors (torso fatigue). During fatiguing exercises, participants performed isotonic exertions at 60% of individual capacity at 12 repetitions/min.

2.7 Model simulation and analysis

The flow of model simulation here was the same as described earlier for our 2D balance control model (Qu et al. 2007).

Table 1. Glossary of COP-based dependent measures.

Acronym	Description	Units
RMS	Root mean square distance	mm
MV	Mean velocity	mm/s
CFREQ	Centroidal frequency	Hz
FREQD	Frequency dispersion	–
TT	Transition time	s
TA	Transition amplitude	mm^2
H_S	Short-term scaling exponent	–
H_L	Long-term scaling exponent	–

After specifying the model parameters (by minimising the cost function, Equation (18)), the model was then used to predict both traditional and some statistical mechanics COP-based measures that did not appear in the cost function. The latter were the transition time (A/P TT and M/L TT), transition amplitude (A/P TA and M/L TA), short-term scaling exponent (A/P H_S and M/L H_S) and long-term scaling exponent (A/P H_L and M/L H_L (Collins and DeLuca 1993; Rougier 1999). Descriptions and units of both traditional and statistical mechanics measures are given in Table 1. Note that traditional and statistical mechanics measures derived from COP time series assess fundamentally different aspects of postural control (Norris et al. 2005). Specifying the model using the former, and evaluating it using the latter, was considered a fairly rigorous method to assess the performance of the 3D balance control model. In addition, inclusion of both pre- and post-fatigue COP data allowed for assessment of the model over a broader range of circumstances.

Quantitative evaluation of the model was undertaken by comparing simulated COP-based measures with corresponding experimental measures. Specifically, the simulated measures were normalised by their corresponding experimental measures, and 95% confidence intervals of these normalised simulated measures were obtained (i.e. perfect predictions would yield values of unity). These confidence intervals are equivalent to two-tailed t-tests with $\alpha = 0.05$, and differences between the simulated and experimental data are not significant if values of unity were included in the confidence intervals. In addition, normalised errors between simulated and experimental COP-based measures were also calculated and presented to evaluate the model performance in simulating COP-based measures.

Values of the cost function (Equation (18)), which are the scalar errors between simulated and experimental data, were used to assess whether the model simulation ability differed between pre- and post-fatigue conditions. This comparison was done using a one-way ANOVA. Finally, bivariate correlations were determined between the simulated COP-based measures and model parameters.

3. Results

For all traditional COP-based measures, 95% confidence intervals of the normalised simulated values included unity (Figure 5(a)), and means for these were all within the range of 0.9–1.1, or very close to the ideal value of unity. Furthermore, mean normalised errors between simulated and experimental traditional COP-based measures were all $<8\%$ (Table 3). These results suggest that the proposed model could reasonably simulate traditional COP-based measures. In contrast, predictions of statistical mechanics measures were somewhat less favourable. Except for TT, mean values were generally close to unity (Figure 5(b)), and mean normalised errors were ~ 3–66% (Table 3). All confidence intervals for predicted statistical mechanics measures contained unity, though these intervals were quite broad (Figure 5(b)). Among the statistical mechanics measures, H_S was predicted substantially better (i.e. mean near unity, normalised error $<4\%$ and small confidence interval range). A non-significant ($p = 0.14$) effect of fatigue was found on the cost function, which had a mean (SD) value for pre-fatigue data of 0.439 (0.171), and respective values of 0.479 (0.145) and 0.456 (0.140) after ankle and torso fatigue.

Some patterns were evident among the bivariate correlations between model parameters and COP-based measures (Table 4). Random disturbance gains (k_{n1} and k_{n2}) were significantly correlated with all simulated COP-based measures except H_S. In contrast, some model parameters (w_{11}, w_{21} and w_{12}) had no significant correlations with any of the simulated COP-based measures.

Table 2. Summary values of experimental COP-based measures.

		RMS	MV	CFREQ	FREQD	TT	TA	H_S	H_L
A/P	Mean	6.68	10.52	0.549	0.903	0.579	26.33	0.817	0.198
	SD	2.95	3.55	0.139	0.061	0.297	26.23	0.041	0.100
M/L	Mean	6.31	13.08	0.582	0.844	0.477	34.35	0.829	0.148
	SD	2.19	4.95	0.153	0.079	0.122	31.50	0.030	0.109

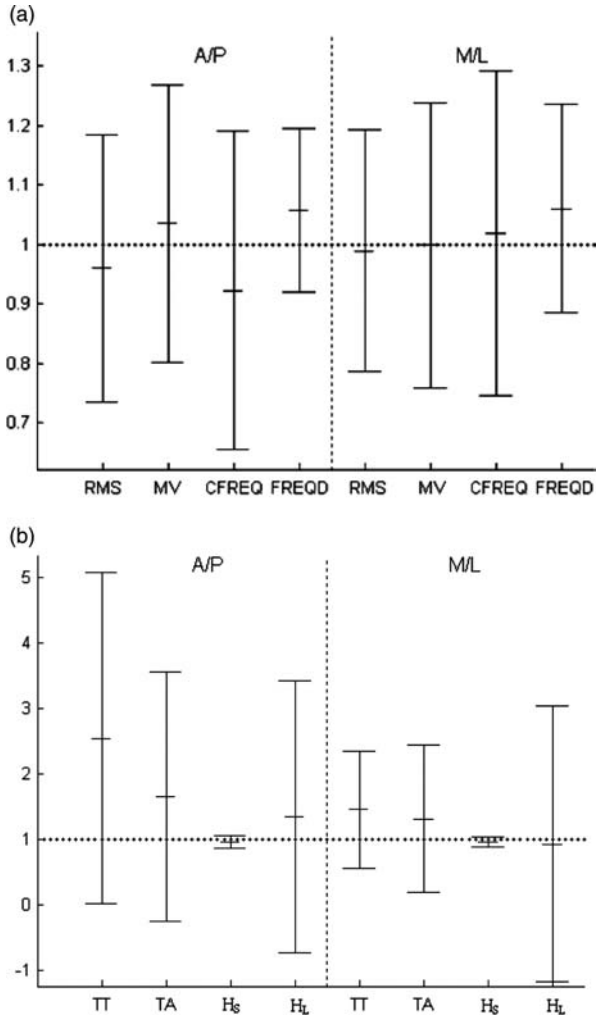

Figure 5. Means and 95% confidence intervals of the normalised simulated COP-based measures (top: traditional measures; bottom: statistical mechanics measures). Dotted horizontal lines indicate unity, or perfect model predictions. Experimental references used for normalisation are given in Table 2.

4. Discussion

In this study, a 3D balance control model based on an optimal control strategy was developed, and evaluated in terms of its ability to simulate postural sway in both the A/P and M/L directions. As COP-based measures are most commonly used to characterise postural sway (Prieto et al. 1996; Peterka 2000; Baratto et al. 2002), we adopted COP-based measures to evaluate the simulation performance of the model. In general, COP-based measures can be classified into three groups: time-domain measures, frequency-domain measures and statistic mechanical measures (e.g. Prieto et al., 1996; Norris et al., 2005). Each of these types was incorporated, including two time-domain measures (RMS and MV), two frequency-domain measures (CFREQ and FREQD) and four statistical mechanics measures (TT, TA, H_S and H_L). Given this range of measures, results obtained from this study can be expected to reasonably account for diverse aspects of balance control mechanisms.

There were no significant differences between any of the simulated traditional measures and their experimental references, and the normalised errors between them were as small as less than 8%. In addition, the simulated measures were fairly consistent, having narrow confidence intervals, despite being generated across a range of participants and for conditions before and after LMF. Good performance was also found overall in predicting statistical mechanics measures given that the simulated and experimental statistical mechanics measures were not significantly different. According to these results, the 3D balance control model appears able to accurately simulate postural sway behaviours. Thus, our initial hypothesis was supported. Such a model may thus be of use to further investigate balance control mechanisms, for example, when individual differences and task conditions (e.g. ageing and LMF) affect balance control.

It is important to note the essential difference between the traditional and statistical mechanics measures derived from COP time series, and that each was used differently here. Experimental values of traditional measures must be available in advance, and were used to calculate the cost function. In contrast, experimental values of the statistical mechanics measures were only used after model specification and simulation. Thus, it seems unlikely that simulated traditional measures and simulated statistical mechanics measures would have the same level of accuracy. This argument may help explain why the widths of the confidence intervals of the statistical mechanics measures were typically larger than those of the traditional measures (Figure 5).

Table 3. Normalised errors (as %) between simulated and experimental COP-based measures.

		RMS	MV	CFREQ	FREQD	TT	TA	H_S	H_L
A/P	Mean	3.9	3.6	7.7	5.8	155.2	65.9	3.6	35.4
	SD	22.3	23.2	26.4	13.6	254.3	191.5	9.0	209.0
M/L	Mean	1.1	0.0	1.9	5.9	45.7	31.4	3.5	7.8
	SD	20.3	23.8	27.0	17.4	90.6	114.3	8.1	213.0

Table 4. Bivariate correlations between model parameters and simulated sway measures.

	w_{11}	w_{21}	w_{31}	w_{41}	w_{51}	k_{n1}	τ_{d1}	w_{12}	w_{22}	w_{32}	w_{42}	w_{52}	k_{n2}	τ_{d2}
A/P RMS	− 0.107	− 0.130	0.007	0.147	0.159	0.314*	0.201*	0.142	− 0.077	− 0.084	− 0.033	− 0.062	0.392*	0.084
A/P MV	0.036	− 0.059	0.297*	− 0.115	− 0.142	0.793*	− 0.076	0.051	0.177	0.183	− 0.195	− 0.196	0.860*	− 0.046
A/P CFREQ	0.152	0.016	0.216*	− 0.271*	− 0.135	0.579*	− 0.047	− 0.057	0.279*	0.217*	− 0.156	− 0.177	0.634*	− 0.095
A/P FREQD	− 0.095	− 0.022	− 0.516*	0.280*	0.369*	− 0.455*	0.662*	0.020	− 0.112	− 0.120	0.032	0.179	− 0.111*	0.172
A/P TT	− 0.038	− 0.152	− 0.433*	0.183	0.513*	− 0.399*	0.676*	0.012	− 0.185	− 0.244*	0.139	0.249*	− 0.236*	0.270*
A/P TA	0.044	− 0.118	0.099	− 0.057	0.065	0.239*	0.119	0.084	0.026	0.027	− 0.098	− 0.074	0.365*	0.045
A/P Hs	0.146	0.058	0.309*	− 0.478*	0.059	0.028	− 0.022	− 0.009	− 0.009	0.152	− 0.081	− 0.036	− 0.033	− 0.148
A/P H_L	− 0.107	− 0.139	− 0.481*	0.311*	0.473*	− 0.358*	0.609*	0.069	− 0.294*	− 0.340*	0.209*	0.243*	− 0.280*	0.306*
M/L RMS	0.031	− 0.089	0.061	0.018	− 0.034	0.411*	0.001	0.047	0.039	− 0.095	− 0.051	0.080	0.458*	0.077
M/L MV	0.037	− 0.059	0.242*	− 0.076	− 0.146	0.748*	− 0.053	0.034	0.211*	0.218*	− 0.217*	− 0.201*	0.892*	− 0.046
M/L CFREQ	− 0.032	0.040	0.161	− 0.043	− 0.111	0.555*	− 0.067	− 0.080	0.259*	0.339*	− 0.158	− 0.274*	0.700*	− 0.132
M/L FREQD	− 0.128	0.092	− 0.391*	0.185	0.282*	− 0.352*	0.228*	− 0.228*	− 0.183	− 0.338*	0.421*	0.405*	− 0.450*	0.407*
M/L TT	0.057	− 0.085	− 0.202*	0.093	0.087	− 0.219*	0.177	− 0.054	− 0.093	− 0.183	− 0.151	0.743*	− 0.336*	0.667*
M/L TA	0.086	− 0.075	0.140	− 0.077	− 0.103	0.518*	− 0.016	0.131	0.085	0.128	− 0.352*	0.081	0.515*	0.119
M/L Hs	0.185	0.074	0.078	− 0.279*	− 0.115	0.102	− 0.082	0.082	− 0.036	0.222*	− 0.349*	0.175	0.000	0.050
M/L H_L	− 0.010	− 0.122	− 0.230*	0.200	0.134	− 0.283*	0.168	− 0.152	− 0.123	− 0.466*	0.286*	0.596*	− 0.304*	0.407*

*Significant ($p < 0.05$) correlations.

Among the statistical mechanics measures, we may note that simulated A/P TT was associated with the largest normalised errors (Table 3). TT accounts for the time when a transition occurs from an open-loop to a closed-loop control scheme. As such, the accuracy of simulated A/P TT could be affected by the feedback loop in the postural control system model. As the feedback component in the proposed postural control system model is the sensory system (Figure 1), the current time-delay model may be too simplistic to account for the full features of the sensory system.

No significant or substantial difference was found in the optimisation cost function across several LMF conditions, suggesting that the ability of the model to simulate COP-based measures may not be affected by LMF. This was expected, as none of the model parameters or subparts of the model were specifically designed to reflect the presence or absence of LMF. LMF affects COP time series, and derived COP-based measures (Corbeil et al. 2003; Lin et al. 2009), yet the model has sufficient degrees of freedom (unspecified model parameters) to account for such changes such that simulation accuracy is not affected.

Several significant correlations were found between model parameters and COP-based measures, and can be used to predict and/or specify how internal postural control changes affect balance control. For example, the sensory delay time at the hip (τ_{d2}) had significantly positive correlations with TT and H_L in both the A/P and M/L directions. An increased TT indicates that the open-loop control scheme has a longer duration, whereas an increased H_L suggests that, over long-term intervals, postural control has become less anti-persistent (Norris et al. 2005). Both a longer open-loop control scheme and less anti-persistent postural control might result in a more unstable postural control system because the body posture tends to be further away from equilibrium. Thus, it might be concluded that when the sensory delay time at the hip increased, the postural control system became more unstable.

Similar analysis can be performed for other model parameters. In general, when the statistical mechanics measures increased, the postural control system tended to become more unstable. However, relationships between the statistical mechanics measures and some model parameters were not always consistent. For example, TA significantly increased with increases in random disturbance gains (k_{n1} and k_{n2}), while TT and H_L significantly decreased. In such cases, it cannot be determined whether larger random disturbance torques would lead to a more unstable postural control system simply by analysing statistical mechanics measures, and, therefore, additional COP-based measures should be considered. For instance, when random disturbance gains became larger, time-domain sway measures significantly increased, indicating

that the projection of the whole body COM moved closer to the boundary of the base of support. Thus, a more unstable postural control system should have larger random disturbance joint torques.

The postural control system is a complex (and in most situations an automatic) control system. It is generally accepted that the neural controller generates active joint control torques according to feedback regarding body orientations to maintain balance. Thus, balance control has usually been analysed from a control perspective (e.g. Johansson et al. 1988; Ishida et al. 1997; Iqbal and Roy 2004). Existing control theories, however, are more effective in solving linear control problems, whereas the postural control system is obviously nonlinear. A 2D single-segment inverted pendulum model has been used most often to represent the human body when modelling balance control because linearisation in such a case is relatively easy. In contrast, 3D balance control, models have been rarely used previously due to the inherent complexity, although such a model may be a more valid representation.

In the present study, a linearised 3D balance control model was developed, in which several assumptions were made during linearisation. These assumptions may lead to limitations. For example, we assumed that during quiet upright stance the lower segment and upper segment rotate in the sagittal and frontal planes, respectively, based on earlier evidence for the use of an ankle and hip strategy to control postural sway in these planes (Winter et al. 1996). This assumption may be an oversimplification, in that postural sway in 3D space is likely to be more complex. However, as discussed earlier, the proposed model was able to accurately simulate and predict COP-based measures, supporting the validity of the assumptions adopted regarding the contributions of the ankle and hip joints, at least in the current experimental context. In other words, the current results support previous findings that the ankle and hip strategies are applied primarily to control postural sway in the sagittal and frontal planes, respectively (McClenaghan et al. 1996; Winter et al. 1996). Therefore, the current approach is considered to provide an increment in modelling and understanding the complex processes involved in human postural control, and serves as a basis for future expanded modelling efforts.

References

Alexandrov AV, Frolov AA, Massion J. 2001. Biomechanical analysis of movement strategies in human forward trunk bending. I. Modeling. Biol Cybern. 84:425–434.

Baratto L, Morasso PG, Re C, Spada G. 2002. A new look at posturographic analysis in the clinical context: sway-density versus other parameterization techniques. Motor Control. 6:246–270.

Chaffin DB, Andersson GBJ, Martin BJ. 1999. Occupational biomechanics. New York: Wiley.

Collins JJ, DeLuca CJ. 1993. Open loop and closed loop control of posture: a random-walk analysis of center of pressure trajectories. Exp Brain Res. 95:308–318.

Corbeil P, Blouin JS, Begin F, Nougier V, Teasdale N. 2003. Perturbation of the postural control system induced by muscular fatigue. Gait Posture. 18:92–100.

Der Leva P. 1996. Adjustments to Zatsiorsky-seluyanov's segment inertia parameters. J Biomech. 29:1223–1230.

Fujisawa N, Tasuda T, Inaoka H, Fukuoka Y, Ishida A, Minamitani H. 2005. Human standing posture control system depending on adopted strategies. Med Biol Eng Comput. 43: 107–114.

Gunther M, Otto D, Muller O, Blickhan R. 2008. Transverse pelvic rotation during quiet human stance. Gait Posture. 27: 361–367.

Hillier ES, Lieberman GJ. 2005. Introduction to operations research. New York: McGraw-Hill. p. 644–652.

Hsu WL, Scholz JP, Schoner G, Jeka JJ, Kiemel T. 2007. Control and estimation of posture during quiet stance depends on multijoint coordination. J Neurophysiol. 97:3024–3035.

Ishida A, Imai S, Fukuoka Y. 1997. Analysis of the posture control system under fixed and sway-referenced support conditions. IEEE T Biomed Eng. 44:331–336.

Iqbal K, Roy A. 2004. Stabilizing PID controllers for a single-link biomechanical model with position, velocity, and force feedback. J Biomech Eng. 126:838–843.

Johansson R, Magnusson M, Akesson M. 1988. Identification of human postural dynamics. IEEE T Biomed Eng. 35: 858–869.

Kuo AD. 1995. An optimal control model for analyzing human postural balance. IEEE T Biomed Eng. 42:87–101.

Lin D, Nussbaum MA, Seol H, Singh NB, Madigan ML, Wojcik LA. 2009. Acute effects of localized muscle fatigue on postural control and patterns of recovery during upright stance: influence of fatigue location and age. Euro J Appl Physiol. 106:425–434.

Maurer C, Peterka RJ. 2005. A new interpretation of spontaneous sway measures based on a simple model of human postural control. J Neurophysiol. 93:189–200.

McClenaghan BA, Williamsb HG, Dickerson J, Dowda M, Thombs L, Eleazer P. 1996. Spectral characteristics of aging postural control. Gait Posture. 4:112–121.

Norris JA, Marsh AP, Smith IJ, Kohut RI, Miller ME. 2005. Ability of static and statistical mechanics posturographic measures to distinguish between age and fall risk. J Biomech. 38:1263–1272.

Peterka RJ. 2000. Postural control model interpretation of stabilogram diffusion analysis. Biol Cybern. 82:335–343.

Prieto TE, Myklebust JB, Hoffmann RG, Lovett EG, Myklebust BM. 1996. Measures of postural steadiness: differences between healthy young and elderly adults. IEEE T Biomed Eng. 43:956–966.

Qu X. 2010. Physical load handling and listening comprehension effects on balance control. Ergonomics. 53: 1461–1467.

Qu X, Nussbaum MA. 2009a. Effects of external loads on balance control during upright stance: experimental results and model-based prediction. Gait Posture. 29:23–30.

Qu X, Nussbaum MA. 2009b. Evaluation of the roles of passive and active control of balance using a balance control model. J Biomech. 42:1850–1850.

Qu X, Nussbaum MA, Madigan ML. 2007. A balance control model of quiet upright stance based on an optimal control strategy. J Biomech. 40:3590–3597.

Qu X, Nussbaum MA, Madigan ML. 2009. Model-based assessments of the effects of age and ankle fatigue on the control of upright posture in humans. Gait Posture. 30: 518–522.

Robertson DGE, Caldwell GE, Hamill J, Kamen G, Whittlesey SN. 2004. Research methods in biomechanics. Champaign (IL): Human Kinetics.

Rougier P. 1999. Automatic determination of the transition between successive control mechanisms in upright stance assessed by modeling of the center of pressure. Arch Physiol Biochem. 107:35–42.

van der Kooij H, Jacobs R, Koopman B, Grootenboer H. 1999. A multisensory integration model of human stance control. Biol Cybern. 80:299–308.

Winter DA, Prince F, Frank JS, Powell C, Zabjek KF. 1996. Unified theory regarding A/P and M/L balance in quiet stance. J Neurophysiol. 75:2334–2343.